Guaranteed Stability of Haptic Systems with Nonlinear Virtual Environments

Brian E. Miller, *Member, IEEE*, J. Edward Colgate, *Member, IEEE*, and Randy A. Freeman, *Member, IEEE*

***Abstract*—Design of haptic systems that guarantee stable interaction is a challenging task. Virtual environments are typically highly nonlinear—resulting in a nonpassive discrete-time model. This paper will investigate how nonlinear mass/spring/damper virtual environments can be designed to guarantee the absence of oscillations and other chaotic behavior in the signal presented to the human operator. In particular, delayed and nondelayed implementation of the mass/spring/damper virtual environment is considered, revealing a nonintuitive result with regard to the allowable *local* stiffness.**

***Index Terms*—Haptics, human/machine interface, nonlinear virtual environments, passivity, stability.**

I. Introduction

STABILITY is a key design consideration in haptic systems because unwanted oscillations are distracting and potentially unsafe for the human operator. Ensuring stability is a challenging proposition, however, because haptic environments are generally highly nonlinear. Here we are concerned with nonlinear impedance characteristics, which include discontinuous jumps where appropriate. A variety of other factors, including sampling and sensor quantization, tend to excite oscillations. Another complicating factor is that haptic systems are necessarily in direct feedback with human operators.

The stability of haptic systems was first addressed by Minsky *et al.* [16]. The effects of sample-and-hold were approximated by a continuous-time, time-delayed model, and the Nyquist stability criterion was used to place an upper bound on the sample-time T. In addition, numerical simulation was used to explore the effects of varying the mass, stiffness and damping parameters of the virtual environment. From the simulations it was observed that the maximum sampling period T (for system stability) is linearly related to $1/K$, linearly related to viscosity B over a wide range, eventually becoming nonlinear, and is not related to mass when the mass is larger than a specified threshold. The general conclusion drawn from these observations was that a slow update-rate can be very restrictive for environment design.

Manuscript received September 14, 1999. This paper was recommended for publication by Associate Editor Y. Xu and Editor S. Salcudean upon evaluation of the reviewers' comments. This paper was presented in part at the IEEE International Conference on Robotics and Automation, Detroit, MI, 1999.

B. E. Miller is with Computer Motion, Inc., Goleta, CA 93117 USA.

J. E. Colgate is with the Department of Mechanical Engineering, Northwestern University, Evanston, IL 60208 USA (e-mail: colgate@northwestern.edu).

R. A. Freeman is with the Department of Electrical and Computer Engineering, Northwestern University, Evanston, IL 60208 USA (e-mail: freeman@ece.nwu.edu).

Publisher Item Identifier S 1042-296X(00)11395-3.

This early study, and several that followed it, assumed a particular model of human dynamics. For instance, Gillespie [7] modeled the human as a second-order linear time-invariant system. His work went further to propose an observer for the human model that made use of real-time data collected by the haptic hardware. Nonetheless, the time-varying nature of human operator dynamics has continued to pose a challenge for the design of guaranteed stable haptic systems. For instance, the study in [9] showed that contact stability in teleoperator systems, which are similar to haptic systems, has a dependence on operator grasp.

Colgate *et al.* attempted to avoid explicit modeling of human operator dynamics by establishing the passivity of the haptic display (haptic device, virtual coupling and virtual environment). Their results provided some useful insights, such as the role played by physical damping (excess passivity) in the haptic device, but were limited essentially to linear virtual environments.

The current work extends this basic approach to haptic systems incorporating a broad class of nonlinear and time-delayed virtual environments [14]. In the nonlinear regime, the results are somewhat more restrictive: while passivity of the haptic display is difficult to establish, it is possible to establish cyclopassivity [10] of the haptic display, which means that the net energy gain of the display is zero or decreasing for closed paths in state space. Cyclopassivity is achieved independent of the human operator.

A second stability result follows when we assume that the operator is supplying passive excitation. This result guarantees the absence of oscillations and other persistent behavior in the signal presented to the user. Oscillations have been problematic in several situations, and typically occur when making or breaking contact with a virtual object.

The contributions of the present work, seen in relation to previous efforts, are summarized in Fig. 1. In this figure, shaded regions denote classes of environments[1] considered in previous studies. Delayed and nondelayed regions refer to the environment delay, providing an explicit (delayed) or implicit (nondelayed) environment model. Environments treated by Colgate and Schenkel [5] were classified as stable linear shift-invariant (LSI) environments. The development was taken a step further to show that the result was valid for the addition of a unilateral nonlinearity. Although not explicitly mentioned, the stability condition derived in [5] allows a class of nonpassive linear environments. Tsai *et al.* [18] motivated the significance of the unilateral nonlin-

[1]In this paper, the term *environment* refers to the discrete-time virtual environment. When we speak of the passivity of the environment, this should be understood to be distinct from the passivity of the haptic display, which further includes the haptic device and virtual coupling.

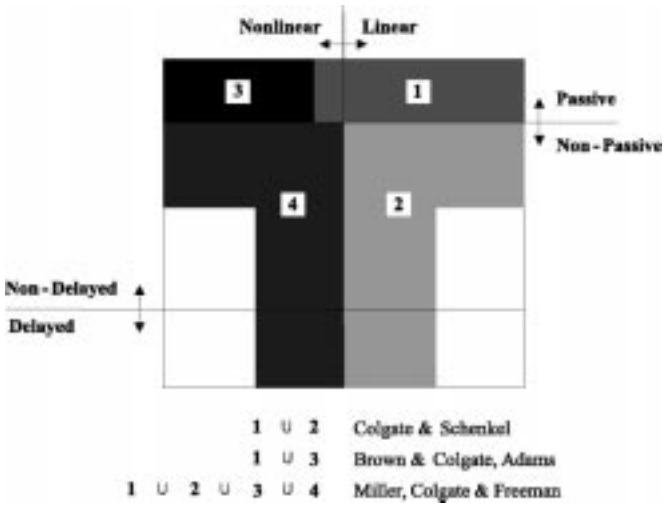

Fig. 1. Classes of virtual environment models.

earity in virtual walls and collisions between rigid bodies, and derived a condition that guarantees absence of oscillations for an LSI system (representing the virtual environment, haptic device and human operator) with a unilateral nonlinearity in feedback. Work by Brown [3], [4] and Adams [1], [2] extended the class of virtual environments to include nonlinear nondelayed environments restricted to be passive, thus losing the portion of nonpassive linear environments once covered. The limitation to passive nonlinear environments is, however, quite restrictive. For instance, the authors have shown that the class of passive nonlinear environments is limited to functions that are nondecreasing (see the Appendix for details). Brown later showed [3] that passive numerical integrators are implicit (nondelayed) making them unlikely candidates for real-time application. This conclusion eliminates complex environments where solving implicit equations in real-time is computationally expensive.

The current work extends existing stability results to include nonpassive nonlinear environments in both delayed and nondelayed form. The importance of this extension is seen in the following applications:

- interaction with surface parametric CAD models [12];
- detection of tissue type in medical simulation [17];
- display of objects with varying textures [16].

All of the above examples are highly nonlinear most likely making the discrete-time model nonpassive. Furthermore, successful real-time implementation often requires delay, which automatically makes the model nonpassive.

In what follows, conditions will be derived for design of delayed and nondelayed nonlinear environments that guarantee the velocity signal from the device to the human goes to zero in steady state and all states are bounded. This implies that an undesirable velocity signal, such as one that is oscillatory, can not be presented to the user.

A nonintuitive result emerges when comparing delayed and nondelayed implementations. For nondelayed environments a bound exists on the *local*[2] negative stiffness the nonlinearity can exhibit. For delayed environments this bound changes sign placing a restriction on the *local* positive stiffness. This result indicates a design choice by implying that if large positive stiffness characteristics are present in the environment, then nondelayed implementation is preferred. However, if the environment exhibits large negative stiffness characteristics (e.g., a snap-action toggle) then delayed implementation is more appropriate.

Recall, unless otherwise stated, reference to delay throughout the paper means environment delay, providing either an implicit (nondelayed) or explicit (delayed) environment model. Implementation of nondelayed environments can take advantage of the allowed large stiffness while still including the effects of computational delay. Extensive details of this development can be seen in [15].

Other attributes that set this result apart from previous work are that general device models can be considered, similar to the development in [1], and that the device model is *exact* [zero-order hold (ZOH) equivalent] instead of a discrete-time approximation. This ensures that conditions derived for the discrete representation directly apply to the original sampled-data system. The distinction between computational delay and environment delay is made, demonstrating that computational delay can be included in the analysis independent of the environment.

II. Stability Concepts

Passivity theory provides a powerful way to describe dynamically coupled systems by focusing on energy transfer [19], [11]. Different levels of passivity exist, and components that contain an *excess* of passivity can be used to compensate for components that exhibit a lack of passivity. The remainder of this section will introduce passivity concepts using the storage function definition.

Definition 1: A system with input u and output y is *passive* if a nonnegative function W (called a storage function) exists, that is a function of the states (x), such that

$$W(x(t)) \le W(x(0)) + \int_0^t y(\tau)u(\tau)\,d\tau - \rho\int_0^t y^2(\tau)\,d\tau - \varphi\int_0^t u^2(\tau)\,d\tau \qquad \forall x \in R^n, \quad x, t \ge 0 \tag{1}$$

with $\rho = \varphi = 0$.

The frequency-domain interpretation is that the Nyquist plot lies in the closed right half plane (RHP) (see Fig. 2).

Definition 2: A system with input u and output y is output strictly passive (OSP) if (1) is satisfied with $\varphi = 0$ and $\rho > 0$.

Output strict passivity is a stronger form of passivity. The frequency-domain interpretation is that the Nyquist plot lies in a disk of radius $1/2\rho$ (see Fig. 2).

Definition 3: A system with input u and output y is input strictly passive (ISP) if (1) is satisfied with $\rho = 0$ and $\varphi > 0$.

Input strict passivity is a stronger form of passivity containing an excess equal to an amount α. The frequency-domain interpretation is that the Nyquist plot lies to the right of the vertical line at φ in the RHP (see Fig. 2).

A component will be referred to as ρ-OSP or φ-ISP with passivity levels ρ and φ, respectively. The discrete-time counter-

[2]*Local* refers to the region near an operating point defined by position, velocity, or acceleration. For example, a bound on the local stiffness refers to a bound on the derivative at the operating point defined by position.

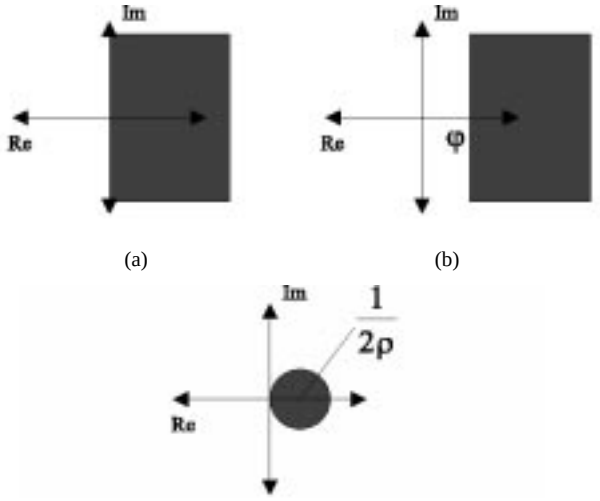

Fig. 2. Frequency-domain interpretations for the different levels of passivity: (a) passive; (b) input strictly passive (ψ-ISP); and (c) ρ-output strictly passive (ρ-OSP).

parts of the above definitions are defined by replacing the integral with a summation [8]. The conditions on the Nyquist plots remain the same. If we define $\Delta W(k) = W(k+1) - W(k)$, we can obtain the incremental version of (1):

$$\Delta W \leq y(k)u(k) - \delta y^2(k) - \varphi u^2(k). \tag{2}$$

III. Problem Formulation

The haptic system considered in this work has four major components: the human operator, haptic device, virtual coupling, and virtual environment. The human (H) and haptic device (D) are continuous-time components while the virtual coupling (V) and virtual environment (E) are discrete-time components. G represents the ZOH equivalent of the human/device feedback loop and z^{-n} denotes computational delay of n time-steps. Fig. 3 illustrates the interaction between these components during implementation.

In what follows, the interaction between the human and haptic display will be examined. This is accomplished by focusing on the velocity signal (v_h) from the haptic display to the human, and guaranteeing that it goes to zero in steady state when the human acts in a passive manner. This eliminates oscillations and other chaotic behavior in the signal presented to the user. The desired stability result is achieved through the following transformation:

$$\hat{G} = \frac{z-1}{Tz}\left[Gz^{-n} + \frac{T}{2\delta}\frac{z^n + z^{n-1} + \cdots + z + 1}{z^n}\right] \tag{3}$$

$$\hat{V} = \frac{z-1}{Tz}\left[V - \frac{T}{2\delta}\frac{z^n + z^{n-1} + \cdots + z + 1}{z^n}\right] \tag{4}$$

$$\hat{E} = E(z)\frac{Tz}{z-1}. \tag{5}$$

The basic idea is to place the system into the form of Fig. 4, whereupon it can be parameterized in terms of passivity levels.

- $\hat{G}$ must be δ-OSP, where δ represents a damping characteristic of the device.

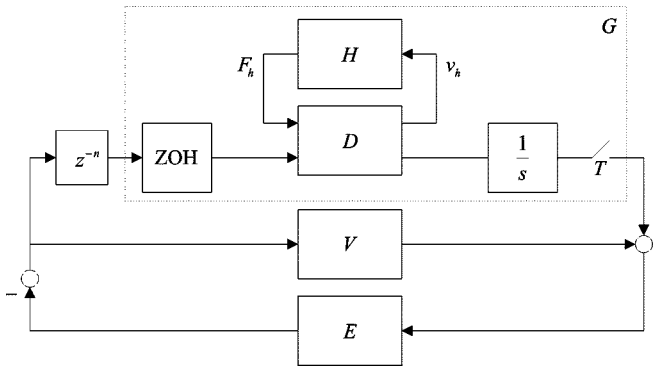

Fig. 3. Haptic system consisting of human (H), haptic device (D), virtual coupling (V), and virtual environment (E).

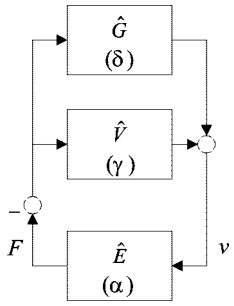

Fig. 4. Transformed haptic system. $\hat{G}$ is the transformed version of human/device, $\hat{V}$ is the transformed version of the virtual coupling, and $\hat{E}$ represents the transformed environment.

- $\hat{V}$ must be γ-OSP.
- $\hat{E} + \alpha$ must be passive (Fig. 5). α is an environment parameter measuring the lack of ISP exhibited by the environment, and can be expressed as a function of inertia, damping and stiffness parameters.

The last term showing up in both (3) and (4) is added to G to achieve a (discrete-time) δ-OSP block once discretization, computational delay and the sample/hold operator are included. So as not to change the dynamics of the original system, this term must be subtracted from the virtual coupling, thus producing (3) and (4) (see [15] for details).

The parallel connection of transformed blocks $\hat{G}$ (δ-OSP) and $\hat{V}$ (γ-OSP) is analogous to resistors in parallel, producing a block that is $\delta\gamma/(\delta+\gamma)$-OSP. Consider a storage function W_1 for the parallel connection of $\hat{G}$ and $\hat{V}$. Since this connection is $\delta\gamma/(\delta+\gamma)$-OSP

$$\Delta W_1 \leq \frac{-\delta\gamma}{\delta+\gamma}v^2 - Fv. \tag{6}$$

Consider a storage function W_2 for the transformed environment block $\hat{E}$ that exhibits a lack of ISP by an amount α.

$$\Delta W_2 \leq \alpha v^2 + Fv. \tag{7}$$

Proposing an energy function $W = W_1 + W_2$

$$\Delta W \leq \left(\alpha - \frac{\delta\gamma}{\delta+\gamma}\right)v^2. \tag{8}$$

Our stability result requires ΔW to be decreasing, therefore

$$\alpha < \frac{\delta\gamma}{\delta+\gamma}. \tag{9}$$

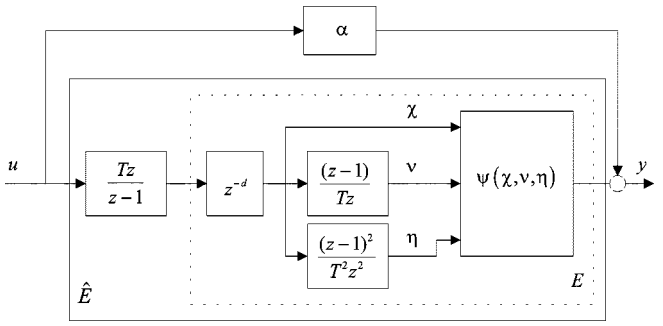

Fig. 5. Transformed environment block. Setting $d = 0$ represents nondelayed implementation while setting $d = 1$ represents delayed implementation.

For $\delta, \gamma > 0$ it follows from (9) that

$$\alpha < \delta. \tag{10}$$

Remark 4: For $\hat{G}$ to be (discrete-time) δ-OSP device D must be (continuous-time) δ-OSP, which is satisfied for a wide range of devices including ones modeled in Lagrangian form with joint flexibility and motor dynamics.

Remark 5: In designing the virtual coupling it is desirable to maximize γ, thus allowing maximum α and permitting as much of a deficit of ISP as possible in the environment. For the commonly used backward difference spring/damper virtual coupling [6], the maximum amount of achievable γ can be shown to equal δ. This implies that $\alpha \leq \delta/2$. On the other hand, from (4) it is clear that if $V = (T/2\delta)((z^n + z^{n-1} + \cdots + z + 1)/z^n)$ then $\hat{V} = 0$, corresponding to $\gamma = \infty$. Therefore, the virtual coupling can in principle be designed to achieve an arbitrarily large γ, however it is unclear what type of perception this will provide. Design of the virtual coupling has proven to be an interesting problem in its own right, and will be considered in future work.

Attention turns to (10), which emerges as the restrictive constraint since δ may represent a physical damping characteristic that is difficult to modify (may require device redesign). This motivates the question of how to determine the α associated with a particular class of environments. The next two sections address this issue and derive a condition on α for delayed and nondelayed implementation in terms of stiffness, damping and inertia characteristics of the virtual environment.

IV. Transformed Environment

This section will focus on the transformed environment block in Fig. 5. The assumption to be verified is that the mapping from u (flow) to y (effort) is passive. Since α is in feedforward with the environment, the environment can exhibit a lack of ISP. This allows nonpassive nonlinear discretization along with computational delay. The remainder of this section will develop conditions on α such that nonlinear mass/spring/damper virtual environments can be displayed, while maintaining the passive mapping from u to y. A nonintuitive result emerges concerning the *local* stiffness slope when considering delayed versus nondelayed implementation.

Nondelayed and delayed environment blocks are obtained by setting $d = 0$ and $d = 1$, respectively, in Fig. 5. The nonlinearity ψ is a mapping from position (χ), velocity (ν), and acceleration (η) to force satisfying the following assumptions.

1) The nonlinearity ψ is piecewise continuous.
2) The nonlinearity ψ is defined such that $\inf_\chi \int_0^\chi \psi(\zeta, 0, 0)d\zeta > -\infty$ (bounded from below in χ).
3) The parameters σ, β, and ϕ defined below are finite.

For nondelayed environments

$$\sigma = \sup_{a \neq b} \frac{\psi(b, 0, 0) - \psi(a, 0, 0)}{a - b} \tag{11}$$

$$\beta = \sup_{\substack{\chi \\ \nu \neq 0}} \frac{\psi(\chi, 0, 0) - \psi(\chi, \nu, 0)}{\nu} \tag{12}$$

$$\phi = \sup_{\substack{\chi \\ \eta \neq 0}} \frac{|\psi(\chi, \nu, 0) - \psi(\chi, \nu, \eta)|}{|\eta|}. \tag{13}$$

For delayed environments

$$\sigma = \sup_{a \neq b} \frac{\psi(a, 0, 0) - \psi(b, 0, 0)}{a - b} \tag{14}$$

$$\beta = \sup_{\substack{\chi \\ \nu \neq 0}} \frac{|\psi(\chi, 0, 0) - \psi(\chi, \nu, 0)|}{|\nu|} \tag{15}$$

$$\phi = \sup_{\substack{\chi \\ \eta \neq 0}} \frac{|\psi(\chi, \nu, 0) - \psi(\chi, \nu, \eta)|}{|\eta|}. \tag{16}$$

These parameters represent stiffness, damping, and inertial properties of the nonlinearity.

Theorem 6: Under Assumptions 1)–3) the condition that guarantees passivity for nondelayed and delayed environments

$$\alpha \geq \frac{1}{2}\sigma T + \beta + \frac{2\phi}{T}. \tag{17}$$

□

The assumptions on the nonlinearity are consistent with physical intuition and provide the designer with an extensive class of environments. Assumption 2 provides a lower bound on the amount of potential energy that can be stored in the system. Definitions of σ, β, and ϕ differ for delayed and nondelayed implementation. The most intriguing difference is that the slope of the stiffness parameter changes sign.

Damping restrictions change from a single to a double sided sector when delay is introduced. This is due to the fact that the Nyquist curve of a delay passes through both $+1$ and -1, indicating the need for an absolute value (i.e., double-sided sector) on the damping term to satisfy the passivity condition.

The inertial property of the nonlinearity is subject to a double-sided sector condition for both delayed and nondelayed implementation. Compare this to an environment where the nonlinearity is affine in the acceleration term η

$$\psi(\chi, \nu, \eta) - \psi(\chi, \nu, 0) = m\eta. \tag{18}$$

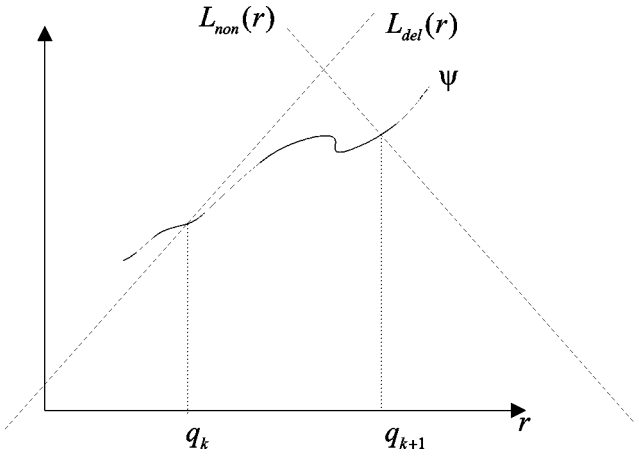

Fig. 6. Function $L(r)$ bounding the nonlinearity over the interval $(q_k \rightarrow q_{k+1})$. The slope changes depending on whether the implementation is delayed or nondelayed.

For nondelayed implementation, a less restrictive condition emerges

$$\alpha \geq \frac{\sigma T}{2} + \beta + \frac{2}{T}\max(0, -m). \tag{19}$$

The above inequality reveals that for positive mass values the last term disappears, whereas for negative mass values we recover (17) with $\phi = |m|$. For the delayed case, an interesting result is found. For positive mass values, (17) is observed. However, for negative mass values it can be determined from the Nyquist plot of the inertia block that the condition becomes even less conservative by almost a factor of two, indicating that for delayed implementation negative mass values help enhance passivity.

Intuition for the difference in the stiffness parameter σ is more difficult to obtain. The implication is that if the environment exhibits large positive stiffness then nondelayed[3] implementation is preferred if computationally feasible. On the other hand, if large *local* negative stiffness is present it may violate the bound for the nondelayed case indicating that a delayed implementation is necessary—a result contrary to the belief that delay is always destabilizing and should be avoided.

Applying passivity tools to the environment requires an upper bound be placed on the change of energy such that it is less than or equal to $y_k u_k$. For delayed implementation, with the change in energy represented by area under the curve (Fig. 6), one looks ahead at the change in energy over the interval $(q_k \rightarrow q_{k+1})$ requiring a line of positive slope to bound the curve from above. For nondelayed implementation, one looks back at the energy change over the interval requiring a line of negative slope to bound the curve from above.

V. Proof

This section provides proof of the passive mapping from u to y for both nondelayed and delayed implementation. Candidate storage functions are proposed and verified leading to the expressions for σ, β, and ϕ stated in the previous section.

Standard state space form for nondelayed implementation is determined from Fig. 5 setting $d = 0$. Introducing states $q_k = \chi_{k-1}$ and $p_k = u_{k-1}$

$$q_{k+1} = q_k + Tu_k \tag{20}$$
$$p_{k+1} = u_k \tag{21}$$
$$y = \alpha u_k + \psi(\chi_k, \nu_k, \eta_k) \tag{22}$$
$$= \alpha u_k + \psi\left(q_k + Tu_k, u_k, \frac{1}{T}[u_k - p_k]\right)$$
$$= \alpha u_k + \psi(q_{k+1}, \nu_k, \eta_k). \tag{23}$$

The potential energy in the environment is defined as

$$U(q) = \int_0^q \psi(\zeta, 0, 0)\, d\zeta - \inf_{\chi} \int_0^{\chi} \psi(\zeta, 0, 0)\, d\zeta \tag{24}$$

and from Assumption 2 is nonnegative and finite.

For the nondelayed case we propose the storage function

$$W(q, p) = \frac{1}{T}\left[U(q) + \frac{1}{2}\phi p^2\right] \tag{25}$$

which we recognize as essentially the sum of the potential and kinetic energy of the environment.

Standard state space form for delayed implementation is determined from Fig. 5 setting $d = 1$. Introducing states $q_k = \chi_k$, $p_k = u_{k-1}$, and $s_k = p_{k-1}$

$$q_{k+1} = q_k + Tu_k \tag{26}$$
$$p_{k+1} = u_k \tag{27}$$
$$s_{k+1} = p_k \tag{28}$$
$$y_k = \alpha u_k + \psi\left(q_k, p_k, \frac{1}{T}[p_k - s_k]\right)$$
$$= \alpha u_k + \psi(q_k, \nu_k, \eta_k). \tag{29}$$

We propose the storage function

$$Y(q, p, s) = \frac{1}{T}U(q) + \left(\frac{1}{T}\phi + \frac{1}{2}\beta\right)p^2 + \frac{1}{2T}\phi s^2. \tag{30}$$

Except for the nonlinear term, the expression is quadratic in the states implying it is nonnegative. The term of interest includes the nonlinearity where we seek a function $L(r)$ such that

$$\frac{1}{T}\int_{q_k}^{q_{k+1}} \psi(\zeta, 0, 0)\, d\zeta \leq \frac{1}{T}\int_{q_k}^{q_{k+1}} L(\zeta)\, d\zeta. \tag{31}$$

Recall passivity expressions (1) and (2), where the terms are quadratic in the input and output variables. For $L(r)$ to be valid, it must be in the form of a quadratic when integrated. Consider function L representing a line of slope σ intersecting the nonlinearity at the current time-step k. Notice that in the nondelayed case the nonlinearity is a function of $q_{k+1} = \chi_k$, and in the delayed case the nonlinearity is a function of $q_k = \chi_{k-1}$.

Graphically in Fig. 6, we can see that for $L(r)$ to bound the nonlinearity over the interval $(q_k \rightarrow q_{k+1})$, the slope must change sign between the cases. It is also clear from the graph-

[3]Recall that an implicit (nondelayed) environment does not imply no delay in the system. Computational delay can still be accounted for by setting $n = 1$ in Fig. 3.

ical representation why in the nondelayed case *local* positive stiffness can be arbitrarily large and for the delayed case *local* negative stiffness can be arbitrarily large. Therefore, the function used in the analysis to bound the nonlinearity is defined in the following manner, for nondelayed and delayed implementation:

$$L_{\text{non}}(r) = \psi(q_{k+1}, 0, 0) + \sigma(q_{k+1} - r) \tag{32}$$

$$L_{\text{del}}(r) = \psi(q_k, 0, 0) + \sigma(r - q_k). \tag{33}$$

A. Nondelayed Implementation

Calculating $\Delta W = W(k+1) - W(k)$

$$\Delta W = \frac{1}{T}\int_{q_k}^{q_{k+1}} \psi(\zeta, 0, 0)\, d\zeta + \frac{1}{2}[\phi p^2(k+1) - \phi p^2(k)]. \tag{34}$$

Starting with the definition of σ (11), and multiplying both sides by $(q_{k+1} - r)\, dr \geq 0$

$$\psi(r, 0, 0)\, dr \leq \psi(q_{k+1}, 0, 0)\, dr + \sigma(q_{k+1} - r)\, dr = L(r)\, dr \tag{35}$$

thus satisfying condition (31) for $L = L_{\text{non}}$. Evaluating the right-hand side of (31), using $L = L_{\text{non}}$, and substituting state equation (20)

$$\frac{1}{T}\int_{q_k}^{q_{k+1}} L(r)\, dr = \psi(q_{k+1}, 0, 0)u_k + \frac{\sigma T}{2} u_k^2. \tag{36}$$

Expanding the term

$$\begin{aligned}&\psi(q_{k+1}, 0, 0)\\ &\quad = \psi(q_{k+1}, \nu_k, \eta_k) + \psi(q_{k+1}, \nu_k, 0)\\ &\qquad - (\psi(q_{k+1}, \nu_k, \eta_k) + \psi(q_{k+1}, \nu_k, 0) - \psi(q_{k+1}, 0, 0))\end{aligned} \tag{37}$$

we can express the right-hand side of (36) as follows:

$$\begin{aligned}&\left(\psi(q_{k+1}, \nu_k, \eta_k)u_k + \frac{\sigma T}{2}u_k^2\right)\\ &\qquad - (\psi(q_{k+1}, \nu_k, 0) - \psi(q_{k+1}, 0, 0))u_k\\ &\qquad - (\psi(q_{k+1}, \nu_k, \eta_k) - \psi(q_{k+1}, \nu_k, 0))u_k.\end{aligned} \tag{38}$$

We will now consider each term of the above expression separately. Substituting (23) into the first term produces

$$y_k u_k - \left(\alpha - \frac{\sigma T}{2}\right) u_k^2 \tag{39}$$

providing the $y_k u_k$ term and a relationship between α and σ. Focusing on the second term, we see that the nonlinearity ψ is a function of $\nu_k = u_k$, introducing a u_k^2 term. This implies the existence of a single sector bound (12)

$$-(\psi(q_{k+1}, \nu_k, 0) - \psi(q_{k+1}, 0, 0))u_k \leq \beta u_k^2. \tag{40}$$

For the third term, the parameter being varied (η_k) is different from u_k so we assume a double-sided sector will exist for inertia. Bounding it by its absolute value [recall expression (13)]

$$-(\psi(q_{k+1}, \nu_k, \eta_k) - \psi(q_{k+1}, \nu_k, 0))u_k \leq \phi |u_k||\eta_k|. \tag{41}$$

Substituting $\eta_k = (1/T)[u_k - p_k]$, replacing $-(\phi/T)p_k u_k \leq |(\phi/T)p_k u_k|$ and applying Young's inequality

$$\phi |u_k||\eta_k| \leq \frac{3}{2T}\phi u_k^2 + \frac{1}{2T}\phi p_k^2. \tag{42}$$

Substituting (39), (40), and (42) into ΔW

$$\begin{aligned}\Delta W \leq y_k u_k - \left(\alpha - \frac{\sigma T}{2} - \beta\right) u_k^2 + \frac{3}{2T}\phi u_k^2\\ + \frac{1}{2T}\phi p_k^2 + \frac{1}{2T}[\phi p_{k+1}^2 - \phi p_k^2].\end{aligned} \tag{43}$$

Recall $p_{k+1} = u_k$

$$\Delta W \leq y_k u_k - \left(\alpha - \frac{\sigma T}{2} - \beta - \frac{2\phi}{T}\right) u_k^2. \tag{44}$$

To guarantee that $\Delta W \leq y_k u_k$ for passivity, we need

$$\alpha \geq \frac{\sigma T}{2} + \beta + \frac{2\phi}{T}. \tag{45}$$

B. Delayed Implementation

Calculating ΔY

$$\begin{aligned}\Delta Y = \frac{1}{T}\int_{q_k}^{q_{k+1}} \psi(\zeta, 0, 0)\, d\zeta + \left(\frac{1}{T}\phi + \frac{1}{2}\beta\right)\\ \cdot [p^2(k+1) - p^2(k)] + \frac{1}{2T}\phi[s^2(k+1) - s^2(k)].\end{aligned} \tag{46}$$

Starting with the definition of σ (14), and multiplying both sides by $(r - q_k)\, dr \geq 0$

$$\psi(r, 0, 0)\, dr \leq \psi(q_k, 0, 0)\, dr + \sigma(r - q_k) dr = L(r)\, dr \tag{47}$$

thus satisfying condition (31) for $L = L_{\text{del}}$. Evaluating the left-hand side of (31), using $L = L_{\text{del}}$, and substituting state equation (26)

$$\frac{1}{T}\int_{q_k}^{q_{k+1}} L(r)\, dr = \psi(q_k, 0, 0)u_k + \frac{\sigma T}{2} u_k^2. \tag{48}$$

Expanding the term

$$\begin{aligned}\psi(q_k, 0, 0) = \psi(q_k, \nu_k, \eta_k) + \psi(q_k, \nu_k, 0)\\ - (\psi(q_k, \nu_k, \eta_k) + \psi(q_k, \nu_k, 0) - \psi(q_k, 0, 0))\end{aligned} \tag{49}$$

we can express the right-hand side of (36) in the following way:

$$\begin{aligned}&\left(\psi(q_k, \nu_k, \eta_k)u_k + \frac{\sigma T}{2}u_k^2\right) - (\psi(q_k, \nu_k, 0) - \psi(q_k, 0, 0))u_k\\ &\qquad - (\psi(q_k, \nu_k, \eta_k) - \psi(q_k, \nu_k, 0))u_k.\end{aligned} \tag{50}$$

We will now consider each term of the above expression separately. Substituting (29) into the first term produces

$$y_k u_k - \left(\alpha - \frac{\sigma T}{2}\right) u_k^2 \tag{51}$$

providing the $y_k u_k$ term and a relationship between α and σ. Focusing on the second term, we see that the nonlinearity ψ is a function of u_{k-1}, which is multiplied by u_k. Since these signals may be of opposite sign this implies a double-sided sector bound (15). We can bound this term by its absolute value

$$-(\psi(q_k, \nu_k, 0) - \psi(q_k, 0, 0))u_k \leq \beta |p_k||u_k|. \tag{52}$$

Using Young's inequality

$$\beta |u_k||u_{k-1}| \leq \beta \tfrac{1}{2} u_k^2 + \beta \tfrac{1}{2} u_{k-1}^2. \tag{53}$$

For the third term, the parameter being varied (η_k) is different from u_k so we assume a double-sided sector will exist for inertia. Bounding it by its absolute value [recall expression (16)]

$$-(\psi(q_k, \nu_k, \phi_k) - \psi(q_k, \nu_k, 0))u_k \leq \phi |u_k||\eta_k|. \tag{54}$$

Substituting $\eta_k = (1/T)[p_k - s_k]$ and applying Young's inequality

$$\phi |u_k||\eta_k| \leq \frac{\phi}{T} u_k^2 + \frac{\phi}{2T} p_k^2 + \frac{\phi}{2T} s_k^2. \tag{55}$$

Substituting (51), (53), and (55) into ΔY

$$\begin{aligned} \Delta Y \leq\, & y_k u_k - \left(\alpha - \frac{\sigma T}{2}\right) u_k^2 + \beta \frac{1}{2} u_k^2 + \beta \frac{1}{2} u_{k-1}^2 + \frac{1}{T} \phi u_k^2 \\ & + \frac{1}{2T} \phi p_k^2 + \frac{1}{2T} \phi s_k^2 + \frac{1}{T} \phi p_{k+1}^2 - \frac{1}{T} \phi p_k^2 + \frac{1}{2T} \phi s_{k+1}^2 \\ & - \frac{1}{2T} s_k^2 + \frac{1}{2} \beta p_{k+1}^2 - \frac{1}{2} \beta p_k^2. \end{aligned} \tag{56}$$

Recall $p_{k+1} = u_k$

$$\Delta Y \leq y_k u_k - \left(\alpha - \frac{\sigma T}{2} - \beta - \frac{2\phi}{T}\right) u_k^2. \tag{57}$$

To guarantee that $\Delta Y \leq y_k u_k$ for passivity, we need

$$\alpha \geq \frac{\sigma T}{2} + \beta + \frac{2\phi}{T}. \tag{58}$$

It is convenient that the stability result for nondelayed and delayed environments takes the same form, however it is important to note the appropriate definitions for σ, β, and ϕ.

VI. Discussion/Conclusion

The proceeding section derived a condition for α that allows implementation of delayed and nondelayed nonlinear environments. This expression can be used along with

$$\alpha < \delta \tag{59}$$

$$\alpha < \frac{\delta \gamma}{\delta + \gamma} \tag{60}$$

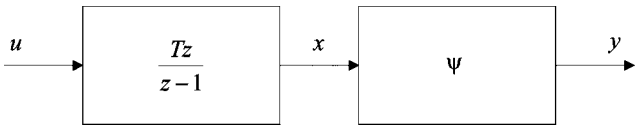

Fig. 7. Virtual environment consisting of an integrator followed by a nonlinearity.

to guide haptic system design in various ways.

For example, suppose we have a haptic device with damping characteristic $\delta > 0$, and would like to determine the class of environments that can be displayed passively. The first step is to quantify δ using a device model or experimentation. Once δ is known, with knowledge that $\alpha < \delta$, we can begin to determine what implications this has on environment design.

Or, consider the task of simulating epidural needle placement. In this task, and many like it, the class of environments is well characterized. Parameters σ, β, and ϕ can be determined based on this characterization. Equation (59) can be used to determine the amount of physical damping required in the device. Once the device has been assembled, the virtual coupling can be designed using (60). The design of the virtual coupling is closely related to the amount of damping (δ) in the device. Assuming a virtual coupling with pure stiffness, it can be shown that $\gamma = \delta KT/(2\delta - KT) > 0$. This is satisfied if $\delta > KT/2$. Therefore, as the damping characteristic δ is reduced, either the virtual coupling stiffness must be reduced or the sampling rate must be increased.

Finally, if a device exists and a desired class of environments is known, then the desired results can be obtained by adjusting the sampling period (T).

Following any of the above design scenarios provides a procedure that allows nonlinear mass/spring/damper environments while guaranteeing stable interaction.

Appendix

The proof that follows will show that a passive mapping from $u(k)$ to $y(k)$, for the system in Fig. 7, exists only if the nonlinearity is nondecreasing. It is important to note that this result occurs due to the discrete nature of the system. A nonlinearity preceded by an integrator in a continuous-time system is not restricted to be nondecreasing to achieve passivity.

Consider a static nonlinearity ψ, where $a > b$ and $\psi(a) < \psi(b)$. The state space representation for the system, introducing state $q_k = x_{k-1}$, takes the form

$$q_{k+1} = q_k + T u_k \tag{61}$$

$$y_k = \psi(q_k + T u_k). \tag{62}$$

Consider an arbitrary storage function $W(q(k))$, which must satisfy the following condition for passivity:

$$0 \leq W(q(k)) \leq W(q(0)) + \sum_{i=1}^{n} y_k u_k. \tag{63}$$

If we apply the input sequence u (column 2 of Table I), we obtain the input/output product in column 5. After the term for $k = 0$, the input/output terms can be grouped together ($k = 1$

TABLE I
INPUT/OUTPUT SEQUENCE

k	u	x	y	yu
0	a	a	$\psi(a)$	$a\psi(a)$
1	$-\tau$	b	$\psi(b)$	$-\tau\psi(b)$
2	τ	a	$\psi(a)$	$\tau\psi(a)$
3	$-\tau$	b	$\psi(b)$	$-\tau\psi(b)$
2	τ	a	$\psi(a)$	$\tau\psi(a)$
$\vdots$	$\vdots$	$\vdots$	$\vdots$	$\vdots$

with $k = 2$, $k = 3$ with $k = 4$, etc.) to produce an infinite contribution from the term $\tau(\psi(a) - \psi(b))$. Since the nonlinearity is defined such that $\psi(a) < \psi(b)$, the contribution from the term $\tau(\psi(a) - \psi(b))$ is negative, eventually converging to $-\infty$ violating condition (63).

If we restrict the nonlinearity to be nondecreasing, we see that this problem is avoided. In fact, we can propose the following storage function:

$$U(q) = \frac{1}{T}\left[\int_0^q \psi(\zeta)\,d\zeta - \inf_x \int_0^x \psi(\zeta)\,d\zeta\right]. \qquad (64)$$

Since the nonlinearity is nondecreasing the following inequality is satisfied:

$$\frac{1}{T}\int_{q_k}^{q_{k+1}} \psi(\zeta)\,d\zeta \le \psi(q_{k+1})[q_{k+1} - q_k] = y_k u_k \qquad (65)$$

revealing that the system is passive.

ACKNOWLEDGMENT

The authors would like to acknowledge B. Gillespie for his thorough review of this paper and his many insightful comments.

REFERENCES

[1] R. Adams and B. Hannaford, "A two-port framework for the design of unconditionally stable haptic interfaces," in *Proc. IEEE/RSJ Int. Conf. Intelligent Robots and Systems*, 1998.
[2] ——, "Stability and performance of haptic displays: Theory and experiments," in *Proc. Int. Mechanical Engineering Congress and Exhibition*, vol. 64, Nov. 1998, pp. 227–234.
[3] J. M. Brown and J. E. Colgate, "Minimum mass for haptic display simulations," in *Proc. Int. Mechanical Engineering Congress and Exhibition*, vol. 64, Nov. 1998, pp. 85–92.
[4] ——, "Passive implementation of multibody simulations for haptic display," in *Proc. Int. Mechanical Engineering Congress and Exhibition*, vol. 61, Nov. 1997, pp. 85–92.
[5] J. E. Colgate and G. G. Schenkel, "Passivity of a class of sampled-data systems: Application to haptic interfaces," *J. Robot. Syst.*, vol. 14, no. 1, pp. 37–47, 1997.
[6] J. E. Colgate, M. C. Stanley, and J. M. Brown, "Issues in the haptic display of tool use," in *Proc. IEEE/RSJ Int. Conf. Intelligent Robots and Systems*, 1995.
[7] R. B. Gillespie and M. R. Cutkosky, "Stable user-specific haptic rendering of the virtual wall," in *Proc. Int. Mechanical Engineering Congress and Exhibition*, vol. 61, Nov. 1995, pp. 85–92.
[8] G. C. Goodwin and K. S. Sin, *Adaptive Filtering Prediction and Control*. Englewood Cliffs, NJ: Prentice-Hall, 1984, pp. 489–495.
[9] B. Hannaford and R. Anderson, "Experimental and simulation studies of hard contact in force replecting teleoperation," in *Proc. Int. Conf. Robotics and Automation*, vol. 1, 1988, pp. 584–589.
[10] D. J. Hill and P. J. Moylan, "Dissipative dynamical systems: Basic input-output and state properties," *J. Franklin Inst.*, vol. 309, no. 5, pp. 327–357, 1980.
[11] ——, "Connections between finite-gain and asymptotic stability," *IEEE Trans. Automat. Contr.*, vol. AC-25, no. 5, pp. 931–936, 1980.
[12] J. M. Hollerbach, E. Cohen, W. Thompson, R. Freier, D. Johnson, A. Nahvi, D. Nelson, and T. V. Thompson II, "Haptic interfacing for virtual prototyping of mechanical CAD designs," in *Proc. DETC ASME Design Engineering Technical Conf.*, May 1997, pp. 375–380.
[13] B. E. Miller, J. E. Colgate, and R. A. Freeman, "Passive implementation for a class of static nonlinear environments," in *Proc. Int. Conf. Robotics and Automation*, May 1999, pp. 2937–2942.
[14] ——, "Environment delay in Haptic systems," in *IEEE Int. Conf. Robotics and Automation*, vol. 2, San Francisco, CA, 2000, pp. 2434–2439.
[15] B. E. Miller, "Stability of Haptic system with nonpassive virtual environments," Ph.D. dissertation, Northwestern Univ., Evanston, IL, 2000.
[16] M. Minsky, M. Ouh-Young, and O. Steele, "Feeling and seeing: Issue in force display," *ACM Trans. Comput.–Human Interactions*, vol. 24-2, pp. 235–243, 1990.
[17] E. Scilingo, D. De Rossi, A. Bicchi, and P. Iacconi, "Haptic display for replication for rheological behavior of surgical tissues: Modeling, control and experiments," in *Proc. Int. Mechanical Engineering Congress and Exhibition*, Dallas, TX, 1997.
[18] J. C. Tsai and J. E. Colgate, "Stability of discrete time systems with unilateral nonlinearities," in *Proc. Int. Mechanical Engineering Congress and Exhibition*, San Francisco, CA, 1995.
[19] J. C. Willems, "Dissipative dynamical systems—Part I: General theory," *Arch. Rational Mech. Anal.*, vol. 45, pp. 321–351, 1972.

Brian E. Miller (M'01) received the B.S. degree in electrical engineering and the B.S. degree in computer engineering from Iowa State University, Ames. He received the M.S. and Ph.D. degrees in mechanical engineering from Northwestern University, Evanston, IL, in December 1998 and December 2000, respectively.

He joined the research and development group at Computer Motion, Inc., Santa Barbara, CA, specializing in medical robotics. His research interests include haptic interface, control systems, medical robotics, and teleoperation.

J. Edward Colgate (M'88) received the Ph.D. degree in mechanical engineering from Massachusetts Institute of Technology (MIT), Cambridge, in 1988.

He subsequently joined Northwestern University, Evanston, IL, where he is currently an Associate Professor in the Department of Mechanical Engineering. His principal research interests include cobots, collaborative robots, and haptic interface. In addition to his academic pursuits, he is a founder of CoMoCo, Inc., a leading developer of human interface technologies for the industrial marketplace.

Dr. Colgate has served as U.S. Editor of *Robotics and Computer Integrated Manufacturing*, and as an Associate Editor of the *Journal of Dynamic Systems, Measurement and Control* and the IEEE TRANSACTIONS ON ROBOTICS AND AUTOMATION.

Randy A. Freeman (S'90–M'95) received the B.S. degree in electrical engineering from Cornell University, Ithaca, NY, in 1990, the M.S. degree in electrical engineering from the University of Illionois at Urbana-Champaign in 1992, and the Ph.D. degree in electrical engineering from the University of California at Santa Barbara in 1995.

He is currently an Assistant Professor in the Department of Electrical and Computer Engineering, Northwestern University, Evanston, IL. He has authored several journal articles and book chapters on nonlinear control, robust control, and optimal control. He is co-author (with P.V. Kokotović) of the book *Robust Nonlinear Control Design* (Boston, MA: Birkhauser).

Dr. Freeman received a National Science Foundation Career Award in 1997.